

1 **Dynamics of transparent exopolymer particles (TEP) during**
2 **the VAHINE mesocosm experiment in the New Caledonia**
3 **lagoon**

4
5 **I. Berman- Frank¹, D. Spungin¹, E. Rahav^{1,2}, F. Van Wambeke³, K. Turk-Kubo⁴, T.**
6 **Moutin³**

7
8 [1] {The Mina and Everard Goodman Faculty of Life Sciences, Bar-Ilan University, Ramat
9 Gan, Israel 5290002}

10 [2] {National Institute of Oceanography, Israel Oceanographic and Limnological Research,
11 Haifa, Israel 31080}

12 [3] {Aix Marseille Université, CNRS/INSU, Université de Toulon, IRD, Mediterranean
13 Institute of Oceanography (MIO) UM110, 13288, Marseille, France }

14 [4] {Ocean Sciences Department, University of California, Santa Cruz, 1156 High Street,
15 Santa Cruz, CA, 95064, USA }

16
17 Correspondence to: I. Berman-Frank (ilana.berman-frank@biu.ac.il)

27 **Abstract**

28 In the marine environment, transparent exopolymeric particles (TEP) produced from abiotic
29 and biotic sources link the particulate and dissolved carbon pools and are essential vectors
30 enhancing vertical carbon flux. We characterized spatial and temporal dynamics of TEP
31 during the VAHINE experiment that investigated the fate of diazotroph-derived nitrogen and
32 carbon in three, replicate, dissolved inorganic phosphorus (DIP)-fertilized 50 m³ enclosures in
33 an oligotrophic New Caledonian lagoon. During the 23 days of the experiment, we did not
34 observe any depth dependent changes in TEP concentrations in the three sampled-depths (1,
35 6, 12 m). TEP carbon (TEP-C) content averaged $28.9 \pm 9.3\%$ and $27.0 \pm 7.2\%$ of TOC in the
36 mesocosms and surrounding lagoon respectively and was strongly and positively coupled with
37 TOC during P2 (= days 15-23). TEP concentrations in the mesocosms declined for the first 9
38 days after DIP fertilization (P1 = days 5-14) and then gradually increased during the second
39 phase. Temporal changes in TEP concentrations paralleled the growth and mortality rates of
40 the diatom-diazotroph association of *Rhizosolenia* and *Richelia* that predominated the
41 diazotroph community during P1. By P2, increasing total primary and heterotrophic bacterial
42 production consumed the supplemented P and reduced availability of DIP. For this period,
43 TEP concentrations were negatively correlated with DIP availability and turnover time of DIP
44 (T_{DIP}), while positively associated with enhanced alkaline phosphatase activity (APA) that
45 occurs when the microbial populations are P-stressed. During P2, increasing bacterial
46 production (BP) was positively correlated with higher TEP concentrations, which were also
47 coupled with the increased growth rates and aggregation of the unicellular UCYN-C
48 diazotrophs that bloomed during this period. We conclude that the composite processes
49 responsible for the formation and breakdown of TEP yielded a relatively stable TEP pool
50 available as both a carbon source and facilitating aggregation and flux throughout the
51 experiment. TEP was probably mostly influenced by abiotic physical processes during P1
52 while biological activity (BP, diazotrophic growth and aggregation, export production) mainly
53 impacted TEP concentrations during P2 when DIP-availability was limited.

54

55 **1 Introduction**

56 The cycling of carbon (C) in the oceans is a complex interplay between physical,
57 chemical, and biological processes that regulate the input and the fate of carbon within the
58 ocean. An essential process driving the flux of carbon and other organic matter to depth and
59 enabling long term sequestration and removal of carbon from the atmosphere is the biological

60 pump that drives organic C formed during photosynthesis to the deep ocean. This process,
61 termed export production (Eppley and Peterson, 1979), is facilitated via physical inputs of
62 ‘new’ nutrients (e.g. nitrogen, phosphorus, silica, trace metals, etc.) into the euphotic zone
63 from either external sources (deep mixing of upwelled water, river discharge, dust deposition,
64 and anthropogenic inputs) or via biological processes such as microbial N₂ fixation that
65 converts biologically unavailable dinitrogen (N₂) gas into bioavailable forms of nitrogen and
66 enhances the productivity of oligotrophic oceanic surface waters that are often limited by
67 nitrogen (Capone, 2001; Falkowski, 1997).

68 Marine N₂ fixation is performed by diverse prokaryotic organisms comprised
69 predominantly of autotrophic cyanobacteria and heterotrophic bacteria (Zehr and Kudela,
70 2011). To supply the energetically-expensive process of converting N₂ to ammonia
71 (Mulholland and Capone, 2000; Postgate and Eady, 1988; Stam et al., 1987), these organisms
72 must obtain energy from either photosynthesis (cyanobacteria) or from bioavailable organic
73 carbon compounds within the aquatic milieu (heterotrophic bacteria and mixotrophs). The
74 total organic carbon (TOC) in the ocean contains dynamic particulate (POC) and dissolved
75 organic carbon (DOC) pools. These are supplied by biotic sources and are broken down into
76 organic C-containing marine microgels which include transparent polymeric particles (TEP).
77 TEP are predominantly acidic polysacchridic organic particles ranging in size from ~0.45 to >
78 300 μm and are found in both marine and freshwater habitats (Passow, 2002). Both biotic and
79 abiotic processes form aquatic TEP that are routinely detected by staining with Alcian Blue
80 (Alldredge et al., 1993; Passow and Alldredge, 1995). Abiotic TEP occur by coagulation of
81 colloidal precursors in the pool of dissolved organic matter (DOM) and from planktonic
82 debris (Passow, 2002; Verdugo and Santschi, 2010) that may be stimulated by turbulence or
83 by bubble adsorption (Logan et al., 1995; Passow, 2002; Zhou et al., 1998). Biotically TEP
84 form from extracellular excretion or mucilage in algae and bacteria and from grazing and
85 microbial breakdown of larger marine snow particles [reviewd in (Bar-Zeev et al., 2015;
86 Passow, 2002)].

87 TEPs are light and bouyant (Azetsu-Scott and Passow, 2004). Yet, once formed, TEPs
88 sticky nature enhances and consolidates the formation of larger aggregates such as
89 marine/lake snow providing favorable environments for diverse microorganisms (Engel,
90 2004; Passow, 2002). Sedimentation of TEP associated “hot spots” from the surface are
91 important for transporting particulate organic material and microorganisms to deeper waters
92 (Azam and Malfatti, 2007; Bar-Zeev et al., 2009; Smith and Azam, 1992). During

93 sedimentation, TEP can also function as a direct source of carbon and other nutrients for
94 higher trophic level organisms such as protists, micro-zooplankton, and nekton (Engel, 2004;
95 Passow, 2002).

96 TEP production can be enhanced in late phases of algal blooms and in senescent or
97 nutrient-stressed phytoplankton (Berman-Frank et al., 2007; Engel, 2004; Grossart et al.,
98 1997; Passow, 2002). Thus, TEP in oligotrophic waters provide a source of available carbon
99 to fuel microbial food webs (Azam and Malfatti, 2007) that typically succeed autotrophic
100 blooms. TEP based aggregates or marine snow containing TEP typically with high carbon
101 (C): nitrogen (N) ratios (Berman-Frank and Dubinsky, 1999; Wood and Van Valen, 1990),
102 which can also fuel N₂ fixation by heterotrophic diazotrophs both in oxygenated surface
103 waters and in the aphotic zones (Benavides et al., 2015; Rahav et al., 2013).

104 The VAHINE project was designed to examine the fate/s of ‘newly’-fixed N by
105 diazotrophs or diazotroph-derived N (hereafter called DDN) in the pelagic food web using
106 large mesocosms in the oligotrophic tropical lagoon of New Caledonia where diverse
107 diazotrophic populations have been observed (Biegala and Raimbault, 2008; Bonnet et al.,
108 2016; Dupouy et al., 2000; Garcia et al., 2007; Rodier and Le Borgne, 2008; Rodier and Le
109 Borgne, 2010). One of the major questions addressed during VAHINE was whether
110 diazotroph blooms significantly modify the stocks, fluxes, and ratios of biogenic elements (C,
111 N, P, Si) and the efficiency of carbon export. To this end, the 3 large-volume (~50 m³)
112 mesocosms containing ambient lagoon waters were fertilized with 0.8 μmol L⁻¹ DIP, and
113 multiple parameters were measured inside and outside of the mesocosms for 23 days [details
114 of parameters and experimental setup in Bonnet et al. (2016)]. Within the VAHINE
115 framework, our specific objectives were: 1) to examine the spatial and temporal dynamics of
116 TEP; 2) to determine whether TEP content was regulated by nutrient status in the mesocosms
117 - specifically DIP availability; 3) to examine the relationship between TEP content, particulate
118 and dissolved carbon, and primary or heterotrophic bacterial production; and 4) to elucidate
119 whether TEP provided a source of energy for diazotrophs/bacteria/mixotrophs in mesocosms.

120

121 **2 Methods**

122 **2.1 Study site, mesocosm description, and sampling strategy**

123 Three large-volume (~50 m³) mesocosms were deployed at the exit of the oligotrophic New
124 Caledonian lagoon (22°29.10 S–166°26.90 E), from 13 January 2013 (day 1) to 4 February

125 2013 (day 23). The complete description of the mesocosm design and deployment, as well as
126 the sampling strategy, is detailed in Bonnet et al. (2016). The mesocosms were supplemented
127 with $0.8 \mu\text{mol L}^{-1} \text{KH}_2\text{PO}_4$ (hereafter referred to as DIP fertilization) between day 4 and 5 day
128 of the experiment to promote N_2 fixation. Samples were collected during the early morning of
129 each day for 23 days with a clean Teflon pumping system from 3 selected depths (1 m, 6 m,
130 12 m) in each mesocosm (M1, M2 and M3) and outside (hereafter called 'lagoon waters'-O).
131 Based on the results of different biogeochemical and biological parameters during VAHINE
132 (Berthelot et al., 2015; Bonnet et al., 2015; Turk-Kubo et al., 2015), three specific periods
133 were discerned (see detailed description in section 3.1) within which we have also
134 investigated TEP dynamics: Days 2-4 (P0) are the pre-fertilization days when the DIP
135 concentrations were $0.02\text{-}0.05 \mu\text{mol L}^{-1} \text{PO}_4^{3-}$ and combined DIN were extremely low; days
136 5-14 (P1) –After fertilization on day 5 the PO_4^{3-} concentrations were $\sim 0.8 \mu\text{mol L}^{-1}$ and
137 diazotrophic populations were dominated by diatom-diazotroph associations. The second
138 stage of the experiment (P2) from days 15 to 23 was characterized by simultaneous increase
139 in primary and bacterial production as well as in N_2 fixation rates which averaged 27.7 nmol
140 $\text{N L}^{-1} \text{d}^{-1}$ (Berthelot et al., 2015) and diazotrophic populations comprised primarily by the
141 unicellular UCYN-C (Turk-Kubo et al., 2015).

142 **2.2 TEP quantification**

143 Water samples (100 mL) were gently ($< 150 \text{ mbar}$) filtered through a $0.45 \mu\text{m}$
144 polycarbonate filters (GE Water & Process Technologies). Filters were then stained with a
145 solution of 0.02% Alcian Blue (AB) and 0.06% acetic acid (pH of 2.5). The excess dye was
146 removed by a quick deionized water rinse. Filters were then immersed in sulfuric acid (80%)
147 for 2 h, and the absorbance at 787 nm was measured spectrophotometrically (CARY 100,
148 equipped with an integrated sphere, Varian). AB was calibrated using different volumes of
149 purified polysaccharide GX (Passow and Alldredge, 1995). TEP concentrations ($\mu\text{g gum}$
150 xanthan [GX] equivalents L^{-1}) were measured according to Passow and Alldredge, (1995).
151 Total TEP content in the mesocosms was calculated by integrating the weighted average of
152 the TEP concentrations per depth and multiplying by the specific volume of each mesocosm.
153 To estimate the role of TEP in C cycling, total amount of TEP-C was calculated for each
154 mesocosm, using the volumetric TEP concentrations at each depth, the specific volume per
155 mesocosm, and the conversion of GX equivalents to carbon applying the revised factor of
156 0.63 based on empirical experiments from both natural samples from different oceanic areas
157 and phytoplankton cultures (Engel, 2004).

158 **2.3 Total Organic Carbon (TOC), Particulate Organic Carbon (POC), Dissolved**
159 **Organic Carbon (DOC)**

160 Samples for TOC concentrations were collected in duplicate from 6 m in each
161 mesocosm and in lagoon waters in precombusted sealed glassware flasks, acidified with
162 H₂PO₄ and stored in the dark at 4 °C until analysis. Samples were analyzed on a Shimadzu
163 TOCV analyzer with a typical precision of 2 μmol L⁻¹. Samples for POC concentrations were
164 collected by filtering 2.3 L of seawater through a precombusted GF/F filter (450 °C for 4 h),
165 combusted and analyzed on an EA 2400 CHN analyzer. DOC concentrations were calculated
166 as the difference between TOC and POC concentrations. Fully detailed methodologies and
167 data are available in Berthelot et al. (2015).

168 **2.4 Dissolved inorganic phosphorus (DIP) and alkaline phosphatase activity**
169 **(APA)**

170 The determination of DIP concentrations are detailed in Berthelot et al. (2015). Samples
171 for DIP were collected from each of the three depths in M1, M2 and M3 and lagoon waters
172 (O) in 40 mL glass bottles, and stored in -20 °C until analysis. DIP concentration was
173 determined using a segmented flow analyzer according to Aminot and K  rouel (2007). The
174 alkaline phosphatase activity (APA) was measured from the same depths and sites using the
175 analog substrate methylumbelliferone phosphate (MUF-P, 1 μM final concentration;
176 SIGMA), (Hoppe, 1983). Full details of the measurements and analyses are described in Van
177 Wambeke et al. (2015).

178 **2.5 Chlorophyll a (Chl a), Primary production (PP) and DIP turnover time**

179 Chlorophyll a (Chl *a*) concentrations were determined by the non-acidification method
180 as described in Berthelot et al. (2015). Primary production (PP) rates and DIP turnover time
181 (T_{DIP}, i.e., the ratio of PO₄⁻³ concentration and uptake) were measured using the ¹⁴C/³³P dual
182 labeling method (Duhamel et al., 2006). 60 mL bottles were amended with ¹⁴C and ³³P and
183 incubated for 3 to 4 h under ambient light and temperature. This was followed by the addition
184 of 50 μL of KH₂PO₄ solution (10 mmol L⁻¹) to stop ³³P assimilation. Samples were then kept
185 in the dark to stop ¹⁴C uptake. Samples were filtered on 0.2 μm polycarbonate membrane
186 filters, and counts were done using a Packard Tri-Carb® 2100TR scintillation counter. PP and
187 T_{DIP} were calculated according to Moutin et al. (2002).

188 **2.6 Bacterial production (BP)**

189 Heterotrophic bacterial production (BP) was estimated using the ³H-leucine
190 incorporation technique (Kirchman, 1993), adapted to the centrifuge method (Smith and
191 Azam, 1992). The complete methodology including enumeration of heterotrophic bacterial
192 abundances (BA) by flow cytometry is detailed in Van Wambeke et al. (2015).

193 **2.7 N₂ fixation, diazotrophic abundance and growth rates**

194 N₂ fixation rates were determined daily on ambient waters from mesocosms and the
195 lagoon. Samples were spiked with 99% ¹⁵N₂-enriched seawater (Mohr et al., 2010), incubated
196 *in situ* under ambient light and seawater temperatures as detailed in Berthelot et al. (2015) and
197 Bonnet et al. (2015).

198 Data and protocols of sampling for diazotrophic abundance and calculation of their
199 respective growth rates are detailed fully in Turk-Kubo et al. (2015). Briefly, samples (from 6
200 m only) were collected every other day from the mesocosms, and from the lagoon waters.
201 DNA was extracted and nine diazotrophic phylotypes were identified using quantitative PCR
202 (qPCR). The targeted diazotrophs were two unicellular diazotrophic symbionts of different
203 *Braarudosphaera bigelowii* strains, UCYN-A1, UCYN-A2; free-living unicellular diazotroph
204 cyanobacterial phylotypes UCYN-B (*Crocospaera* sp.), and UCYN-C (*Cyanothece* sp. and
205 relatives); *Trichodesmium* spp.; and three diatom-diazotroph associations (DDAs), *Richelia*
206 associated with *Rhizosolenia* (Het-1), *Richelia* associated with *Hemiaulus* (Het-2), *Calothrix*
207 associated with *Chaetoceros* (Het-3), and a widespread gamma-proteobacterial phylotype γ -
208 24774A11. Abundances are reported as *nifH* copies L⁻¹ as the number of *nifH* copies per
209 genome in these diazotrophs are uncertain. Growth and mortality rates were calculated for
210 individual diazotrophs inside the mesocosms when abundances were higher than the limit of
211 quantification (LOQ) for two consecutive sampling days as detailed in Turk-Kubo et al.
212 (2015).

213 **2.8 Microscopic Analyses**

214 Detailed method for sampling for microscopic analyses is described in Bonnet et al.,
215 (2015). Phytoplankton were visualized using a Zeiss Axioplan (Zeiss, Jena, 6 Germany)
216 epifluorescence microscope fitted with a green (510-560 nm) excitation filter, which targeted
217 the *Richelia* and the UCYN phycoerythrin-rich cells. The diatom-diazotroph association
218 *Rhizosolenia-Richelia* were imaged in bright-field.

219 **2.9 Statistical analyses**

220 Statistical analyses were carried out with XLSTAT, a Microsoft Office Excel based
221 software. A Pearson correlation coefficient test was applied to examine the association
222 between two variables (TEP versus physical, chemical, or physiological variable) after linear
223 regressions or log-transformation of the data. The non-parametric Kruskal–Wallis one-way
224 analysis of variance was applied to compare between TEP dynamics from each of the
225 different phases. A confidence level of 95% (α - 0.05) was used. More details can be found in
226 the supporting information.

227

228 **3 Results and Discussion**

229 **3.1 General context and spatial and temporal dynamics of TEP**

230 The VAHINE experiment was designed to induce and follow diazotrophic blooms and
231 their fate within an oligotrophic environment (Bonnet et al., 2016). Our specific objectives of
232 investigating TEP dynamics were thus examined within the general context and aims of the
233 large experiment. The first stage of the experiment involved the enclosure of the lagoon
234 waters and 3 days of equilibration of the system (P0 – pre-fertilization days 2-4). At this
235 initial stage the total Chl *a* concentrations averaged around 0.2 $\mu\text{g L}^{-1}$ in the lagoon water and
236 in the mesocosms and the phytoplankton consisted of diverse representatives from the
237 cyanobacteria (*Prochlorococcus*, *Synechococcus*, and diatoms such as *Pseudosolenia calcar-*
238 *avis* (Leblanc et al., 2016). During P0, the most abundant members of the diazotrophic
239 community in the lagoon waters were *Richelia-Rhizosolenia* (Het-1), the unicellular UCYN-
240 A1, UCYN-A2, UCYN-C, and the filamentous *Trichodesmium* (Turk-Kubo et al., 2015).

241 Fertilization of the mesocosms with DIP on day 4 stimulated a two-stage response by
242 the diazotrophic community that was further reflected by many of the measured chemical and
243 biological parameters (Berthelot et al., 2015; Bonnet et al., 2015; Bonnet et al., 2016; Turk-
244 Kubo et al., 2015). After fertilization, from day 5 through day 14 (P1), excluding a significant
245 increase in N₂ fixation rates, the functional community-wide biological responses (Chl *a*, PP,
246 BP, BA) remained relatively low and similar to the values for P0 and for P1 in the outside
247 lagoon waters (Berthelot et al., 2015; Leblanc et al., 2016; Van Wambeke et al., 2015). The
248 autotrophic community during P1 was comprised of picophytoplankton such as
249 *Prochlorococcus Synechococcus*, micro and nanophytoplankton including dinoflagellates, and
250 a diverse diatom community (*Chaetoceros*, *Leptocylindrus*, *Cerataulina*, *Guinardia*, and

251 *Hemiaulus*), (Leblanc et al., 2016). Diatom-diazotroph associations (DDAs), predominantly
252 *Richelia-Rhizosolenia* (Het-1) dominated the diazotroph community in the mesocosms (Turk-
253 Kubo et al., 2015) although it still only contributed from 2% to ~8% of the total diatom
254 biomass in P0 and P1 respectively (Leblanc et al., 2016). These DDAs were succeeded during
255 the last 9 days (day 15 to 23 termed P2) by a large bloom of unicellular diazotrophs
256 characterized predominantly as UCYN-C (Turk-Kubo et al., 2015).

257 The final stage of the experiment (P2, days 15-23) was characterized by significantly
258 enhanced values for many biological parameters including N₂ fixation rates, Chl *a*, PP, BA,
259 BP, and particulate organic carbon and nitrogen compared to their respective average values
260 in P1 (Bonnet et al., 2015; Leblanc et al., 2016; Van Wambeke et al., 2015). In all three
261 mesocosms, a significant bloom of UCYN-C developed (day 11 – M1, day 13-M2, day 15-
262 M3) and remained dominant representatives of the diazotroph community until day 23 (Turk-
263 Kubo et al., 2015). The ambient autotrophic community responded to the input of new N, and
264 the transfer of diazotroph derived N was demonstrated and seen in increasing abundance of
265 *Synechococcus*, pico-eukaryotes, and the non-diazotrophic diatoms *Navicula* and *Chaetoceros*
266 spp. (Bonnet et al., 2015; Leblanc et al., 2016; Van Wambeke et al., 2015). Thus the
267 extremely high N₂ fixation rates during this experiment provided sufficient new N to yield
268 high Chl *a* concentrations (> 1.4 µg L⁻¹) and rates of PP (> 2 µmol C L⁻¹ d⁻¹) (Berthelot et al.,
269 2015).

270 **3.1.1 Dynamics of TEP**

271 TEP concentrations for the entire experimental period ranged from ~22 to 1200 µg GX
272 L⁻¹. In each mesocosm and in the lagoon waters (O), the TEP concentrations were similar for
273 the three sampled depths within the 15 m water-column with an overall average of 350 ± 180
274 µg GX L⁻¹ (Fig. S1). Temporally, TEP concentrations generally followed the three distinct
275 periods (P0, P1, P2) that coincided with the described experimental phases characterized from
276 the diazotrophic populations and the biogeochemical and biological (production) parameters
277 (Berthelot et al., 2015; Bonnet et al., 2015; Leblanc et al., 2016; Turk-Kubo et al., 2015; Van
278 Wambeke et al., 2015) (Fig. 1, Fig. S1). Following the enclosure of the lagoon water in the
279 mesocosms (day 2), TEP concentrations increased from the lowest volumetric concentrations
280 (averaging ~ 50 µg GX L⁻¹) measured on day 2 to reach maximum concentrations in each of
281 the mesocosms (average of ~ 800 µg GX L⁻¹) on day 5, ~ 15 h after the mesocosms were
282 fertilized with DIP (Fig. S1, Fig. 1a). From day 5 to day 14 (P1) average TEP content in M2

283 and M3 decreased slightly yet significantly ($p < 0.05$) with the major decline in all
284 mesocosms measured from day 5 to 6 (Fig. 1, Fig. S1, Table S1). From day 15 to 23 (P2) TEP
285 concentrations in all mesocosms increased gradually ($p < 0.05$) over the subsequent 9 days to
286 reach $381 \pm 39 \mu\text{g GX L}^{-1}$ on day 23 (Fig. 1, Table S1).

287 TEP concentrations in the lagoon waters were compared with those in the mesocosms.
288 These showed a similar pattern of increase in TEP during P0 and P2 while the gradual decline
289 in TEP concentrations during P1 was not statistically significant as observed in the
290 mesocosms (Fig. 1, Fig. S1). In the lagoon waters, average TEP concentrations over the whole
291 experimental period day 2 to day 23 were $335 \pm 56 \mu\text{g GX L}^{-1}$. While temporal variations in
292 the three mesocosms were generally statistically significant (Fig. 1, Table S1), the total TEP
293 content calculated for each mesocosm and for an equivalent volume of lagoon water based on
294 average mesocosm volume did not differ significantly when we assessed all data obtained
295 during P1 and P2 (Fig. 2, $p > 0.05$, Kruskal –Wallis analyses of variance). The lack of
296 significant differences in total TEP content in the mesocosms throughout the experiment
297 could reflect the contrasting processes of formation and breakdown that together maintain a
298 relatively stable pool of available TEP.

299 Mechanical processes such as wave turbulence and tidal effects can influence TEP
300 formation and breakdown (and resulting content), (Passow, 2002; Stoderegger and Herndl,
301 1999). Our results indicate no obvious effects of these parameters on TEP content as these
302 were similar in the enclosed mesocosms and the outside lagoon (Fig. 1, Fig. 2). The difference
303 between the TEP in the mesocosms and the lagoon water is significantly different
304 immediately after P addition and only during P1 after P addition and subsequent utilization
305 when declining P availability was correlated with increased TEP concentrations in the
306 mesocosms. TEP concentrations from the lagoon water during P1 did not show any
307 significant trend (Fig. 1, Fig. S1). In the mesocosms, the significant decline in TEP in the first
308 days after P addition is probably due to two factors: a) phytoplankton relieved of P stress will
309 produce less TEP and increase growth rates, b) bacteria will utilize the added P as well as
310 TEP and other organic C sources to grow – so higher TEP consumption and therefore a more
311 significant decline in the mesocosms compared to the outside lagoon, (see below section 3.2).

312 The relative uniformity and stability of TEP within the 15 m water column of both the
313 mesocosms and the lagoon waters reflects the homogeneity of the shallow lagoon system. The
314 variability between the three depths was statistically insignificant in many of the other
315 physical, chemical, and biological features of the mesocosms and the lagoon waters for

316 temperature, salinity, inorganic nutrients (N, P, Si), POC, PON, POP, DOC, Chl *a*, and
317 primary production and heterotrophic bacterial production (Berthelot et al., 2015; Bonnet et
318 al., 2015; Bonnet et al., 2016; Van Wambeke et al., 2015). In contrast to some marine systems
319 where TEP concentrations were correlated with the vertical distribution of Chl *a* or POC (Bar-
320 Zeev et al., 2009; Bar-Zeev et al., 2011; Engel, 2004; Ortega-Retuerta et al., 2009; Passow,
321 2002), the results we obtained here showed no correlation to the vertical (i.e. depth related)
322 autotrophic signatures. Moreover, the similar TEP concentrations at 1, 6, and 15 m do not
323 support a sub-surface maxima in TEP concentrations, stimulated by abiotic aggregation, at the
324 sea-surface top layer as has been reported at 1 m depth in different oceanic areas (Wurl et al.,
325 2011). Abiotic processes of formation and breakdown can be influential yet here we do not
326 see a depth-correlated specific abiotic driver and TEP were evenly distributed within the 15 m
327 water column for all mesocosms (Fig. S1).

328 **3.2 DIP availability, APA, and TEP content.**

329 The average TEP concentrations we measured in the New Caledonian waters are
330 comparable to TEP concentrations reported from other marine environments such as the
331 eastern temperate-subarctic North Atlantic (Engel, 2004), the Ross Sea (Hong et al., 1997),
332 western Mediterranean – Gulf of Cadiz and the Straits of Gibraltar (García et al., 2002; Prieto
333 et al., 2006), the Gulf of Aqaba (northern Red Sea), (Bar-Zeev et al., 2009), in the northern
334 Adriatic Sea (Radić et al., 2005), and in the New Caledonia lagoon (Mari et al., 2007;
335 Rochelle-Newall et al., 2008).

336 While prediction as to the expected TEP concentrations with trophic or productive
337 status is difficult (Beauvais et al., 2003), decreasing availability of dissolved nutrients such as
338 nitrate and phosphate have been correlated with enriched TEP concentrations in both cultured
339 phytoplankton and natural marine systems (Bar-Zeev et al., 2011; Brussaard et al., 2005;
340 Engel et al., 2002; Urbani et al., 2005). In P-limited systems, low Chl *a* concentrations often
341 reflect the nutrient-stressed phytoplankton. As long as light and CO₂ are available, limitation
342 of essential nutrients results in an uncoupling between carbon fixation and growth during
343 which the excess photosynthate can be used to produce carbon-rich compounds including
344 TEP (Berman-Frank and Dubinsky, 1999; Mari et al., 2001; Rochelle-Newall et al., 2008).
345 Moreover, as DIP-availability declines, cells activate P-acquisition pathways and enzymes
346 such as APA to access P from other sources. Thus, and based on previous data (Bar-Zeev et

347 al., 2011), we hypothesized that TEP content would be negatively correlated with autotrophic
348 biomass (Chl *a*) and PP and positively correlated with APA.

349 Mesocosm fertilization on the evening of day 4 enriched the system with ten-fold
350 higher DIP concentrations that were available for microbial utilization throughout the
351 following 8 – 10 days (Berthelot et al., 2015; Bonnet et al., 2016; Leblanc et al., 2016; Van
352 Wambeke et al., 2015). Thus, when DIP concentrations were relatively sufficient during P1,
353 no statistically significant relationship was observed between TEP and POP, DIP, T_{DIP} , Chl *a*,
354 or PP (Table S2). This situation changed with the declining availability of DIP and the shift in
355 the response of the system during P2 from day 15 to 23. During P2 high TEP concentrations
356 were associated with decreasing DIP for each of the mesocosms with an overall negative
357 correlation ($R^2 = 0.23$, $n = 23$, $p = 0.02$), (Fig. 3a). A similar negative trend was obtained
358 between TEP and the turnover time of DIP (T_{DIP}) ($R^2 = 0.28$ $n = 26$, $p = 0.006$), (Fig. 3b).

359 In the South West Pacific, the critical DIP turnover time (T_{DIP}) required for single
360 filaments of *Trichodesmium* to grow is 2 d (Moutin et al., 2005). Here T_{DIP} values lower than
361 1 d, indicative of a strong DIP deficiency, were reached on day 14 in M1, day 19 for M2, and
362 on day 21 for M3. The average T_{DIP} values during P2 were significantly different in each
363 mesocosm, T_{DIP} of 0.5, 1.8, 3.9 d for M1, M2, M3, respectively (Berthelot et al., 2015).
364 Although turnover rates alone do not indicate P deficiency, increasing alkaline phosphatase
365 activity (APA) suggests that the cells were responding to P stress. APA increased rapidly in
366 both M1 and M2 from day 18 (average for M1 and M2 during P2 $\sim 8 \pm 6$ nmol MUF L⁻¹ h⁻¹)
367 and after day 21 in M3 illustrating a biological response of the microbial community to P
368 stress (Van Wambeke et al., 2015). We did not specifically measure TEP production by
369 autotrophic or heterotrophic plankton. Yet, the significant (although indirect relationship)
370 negative correlation of TEP with DIP concentrations and T_{DIP} (Fig. 3a-b) suggests that
371 microbial responses to decreased DIP availability resulted from either 1) an increase in TEP
372 synthesis through higher polysaccharide production rather than biomass which requires higher
373 nutrients (Berman-Frank and Dubinsky, 1999; Wood and Van Valen, 1990) or 2) nutrient
374 limitation inducing greater breakdown of biomass and POM (maybe via programmed cell
375 death) and subsequent abiotic formation of TEP. We obtained a significant semi-logarithmic
376 relationship between TEP and APA ($R^2 = 0.33$ $n = 25$, $p = 0.002$), (Fig. 3c) which implies
377 active TEP formation when DIP concentrations are reduced and APA increases until a
378 saturating point whereby any further increases in APA do not appear to impact TEP
379 concentrations (Fig. 3c). This relationship may not always be valid as APA in the lagoon

380 waters was consistently higher at 1 m than APA measured at 6 and 12 m depths (Van
381 Wambeke et al., 2015), yet TEP concentrations were uniform at all depths (Fig. S1).

382 **3.3 TEP and carbon pools**

383 The size range of TEP spans a range of particles from 0.45 to 300 μm (Alldredge et al.,
384 1993; Bar-Zeev et al., 2015). TEP precursors (0.05 to 0.45 μm size) are formed and broken
385 down in the DOC pool and thus essentially “TEP establish a bridge between DOM (including
386 DOC) and the POM pool” (Engel, 2004). Our data shows a generally stable contribution of
387 TEP to the TOC pool. Excluding day 5, where TEP-C comprised $56.5 \pm 8\%$ of TOC, the %
388 TEP-C was $28.9 \pm 9.3\%$ and $27.0 \pm 7.2\%$ of the TOC in all mesocosms and in the lagoon
389 waters, respectively (Fig. 4a-b).

390 TEP concentrations can be directly and positively correlated with POC (Engel, 2004)
391 and with DOC (Ortega-Retuerta et al., 2009). Yet, TEP concentrations can also be negatively
392 related to POC indicative of low TEP production when POC concentrations are high (Bar-
393 Zeev et al., 2011). In the mesocosms, a significant positive correlation between TEP
394 concentrations and TOC was obtained for all three mesocosms only during P2 ($R^2 = 0.75$,
395 0.73, 0.58 and $p < 0.05$ for M1, M2, M3 respectively), (Fig. 4c, Table S2). This period
396 coincided with the largest gain in total autotrophic and heterotrophic biomass and elevated N_2
397 fixation, PP, and BP rates (Berthelot et al., 2015; Bonnet et al., 2015; Van Wambeke et al.,
398 2015).

399 Although TEP was significantly and positively correlated with TOC in the mesocosms
400 during P2, this was not the case in the Lagoon water (outside the mesocosms) (Table S2) or
401 with either POC or DOC in any mesocosm for either P1 or P2 (Table S2). The absence of any
402 significant correlation between TEP and POC was surprising as TEP are part of the POC pool
403 comprising 40 – 60% of the particulate combined carbohydrates in POC (Engel, 2004; Engel
404 et al., 2012). Furthermore, we did not obtain any significant correlations of TEP and specific
405 components of the dissolved organic matter such as fluorescent dissolved organic matter
406 (FDOM) or chromophoric dissolved organic matter (CDOM) that was coupled to the
407 dynamics of N_2 fixation in the mesocosms (Tedetti et al., 2015). The lack of significant
408 correlation could partially reflect methodological issues. In this experiment [and operationally
409 according to published protocol (Passow and Alldredge (1995))] TEP was measured on 0.45
410 μm filters – so that Alcian Blue stained particles included particles $> 0.45 \mu\text{m}$ while POC was
411 measured on GF/F (nominal pore size 0.7 μm). DOC is typically considered for the $< 0.45 \mu\text{m}$

412 fraction (Thurman, 1985), although here no direct measurements of DOC were made and
413 DOC was obtained by subtracting POC from TOC. Thus, DOC actually covered the $< 0.7 \mu\text{m}$
414 fraction. Our methodology therefore precluded determination of the smaller TEP precursors
415 that would contribute to the DOC and colloidal pools (Villacorte et al., 2015). As such we
416 probably overestimated TEP relative to POC and at the same time underestimated TEP's
417 contribution to the DOC pool (Bar-Zeev et al., 2009). The lacking correspondence between
418 TEP concentrations and the pools of POC and DOC may also result from the uncoupling
419 between formation and breakdown processes. Abiotic processes, will modify relationships
420 obtained between biotic TEP production and recycling (Wurl et al., 2011). Thus, it is feasible
421 that especially during P1 abiotic factors predominated breaking down larger TEP particles
422 into smaller TEP precursors that would be mobilized to the DOC pool and would thus
423 maintain a relatively stable TEP pool although we observed a positive increase in TEP with
424 increased blooms of DDAs (see below section 3.4.1).

425

426 **3.4 Production and utilization of TEP by primary and bacterial populations**

427 Typically TEP are formed by diverse algal and bacterial species (Mari and Burd, 1998)
428 yet are utilized mostly by bacteria and grazers as a rich C source (Azam and Malfatti, 2007;
429 Bar-Zeev et al., 2015; Engel and Passow, 2001). Throughout this experiment (P1 and P2
430 stages) TEP was not significantly correlated to parameters related to autotrophic production
431 such as total Chl *a*, PP, non-diazotrophic diatom or cyanobacterial abundance, or the growth
432 and mortality rates of these populations (Table S2). Furthermore, during P1, no significant
433 relationship between TEP and BA (total or specific for high and low nucleic acid bacteria-
434 HNA or LNA respectively), BP, or division rates was noted in any of the mesocosms (Table
435 S2).

436 This changed during P2 when TEP was positively correlated to the increasing BP for all
437 three mesocosms (Pearson's correlation coefficient $R^2 = 0.63, 0.66, 0.69$ for M1, M2, and M3
438 respectively, $p < 0.05$), (Fig. 5). This contrasted with the relationship in the lagoon water
439 outside the mesocosms where no significant correlation between TEP and BP was noted (Table
440 S2) During P2, TEP was also strongly and positively correlated to TOC, which significantly
441 increased over this time period (Fig. 4c) due to the high production rates of both
442 photosynthetic and heterotrophic bacterial populations. However, although BP and PP were
443 positively associated during P2 [log-log transformation, Fig. 5 and in Van Wambeke et al.
444 (2015)], we found no direct correlation between TEP and PP for either linear (Table S2) or

445 log-transformed regression (not shown). This coupling between PP and BP, while a concurrent
446 association between TEP and BP occurred during P2, indicates TEP may have been utilized by
447 bacteria as a carbon source (Azam, 1998; Ziervogel et al., 2014) or provided a suitable niche
448 for aggregation and proliferation of heterotrophic bacteria.

449 **3.4.1 TEP and diazotrophic populations**

450 Overall N₂ fixation rates were not significantly correlated with TEP concentrations at
451 any time in the experiment (Table S2). Neither could we discern any direct evidence of TEP
452 providing a carbon source for heterotrophic diazotrophs as was found previously in the Gulf
453 of Aqaba where these organisms contributed greatly to the N₂ fixation rates (Rahav et al.,
454 2015). Indeed, no relationship was found between TEP concentrations and the abundance or
455 growth rates of the heterotrophic diazotrophs γ -24774A11 (Moisander et al., 2014). Although
456 these organisms were present throughout the experiment, and increased ~ 4 fold from day 9 to
457 15 especially in M3, they contributed only a small fraction to the total diazotrophic biomass
458 and N₂ fixation rates (Turk-Kubo et al., 2015).

459 Yet, discerning individual diazotroph populations revealed some species-specific
460 correspondence to TEP at certain periods during the experiment. For example, throughout the
461 experiment, net growth rates (i.e., based on differences of *nifH* copies L⁻¹ from day to day) of
462 the DDA *Richelia* (Het-1) associated with *Rhizosolenia* (Turk-Kubo et al., 2015) temporally
463 paralleled TEP concentrations in all mesocosms (Fig. 6a-c, Fig. 6e-f). During both P1 and P2
464 TEP concentrations were positively correlated with the net growth rates of Het-1 ($R^2=0.6$ $P =$
465 0.0001 , $n = 19$ for all mesocosms (Fig. 6d). Although the DDAs dominated the diazotroph
466 community during P1 (primarily Het-1), their overall contribution to diatom biomass in the
467 mesocosm was low with only 2-8% of all diatom biomass (Leblanc et al., 2016). We did not
468 observe an overall relationship between TEP and total diatom biomass throughout VAHINE
469 although diatoms are well known for their TEP production especially when nutrients are
470 limiting and growth rates decline (Fukao et al., 2010; Urbani et al., 2005). Thus, the positive
471 association between TEP and the growth rates of Het-1 and not of the other DDAs Het-2 and
472 Het-3 is intriguing.

473 TEP was also associated with the growth rates of the unicellular UCYN-C diazotrophs
474 that bloomed during P2 and dominated the N₂ fixation rates of this period (Berthelot et al.,
475 2015; Turk-Kubo et al., 2015). During P2, UCYN-C net growth rates were positively
476 correlated with increasing TEP concentrations ($R^2 = 0.65, 0.83, 0.88$ for M1, M2, M3

477 respectively, $p < 0.05$). Furthermore, UCYN-C probably produced an organic matrix possibly
478 also comprised of TEP that aided the formation of large aggregates (100-500 μm) (Fig. 6g-h).
479 These aggregates were predominantly responsible for the enhanced export production ($22.4 \pm$
480 5% of exported POC), (Bonnet et al., 2015; Knapp et al., 2015). High TEP content was
481 obtained from sediment traps on days 15 and 16 (Fig. S1), corresponding to the height of the
482 UCYN-C bloom in the mesocosms (Turk-Kubo et al., 2015) and substantiating the role of
483 TEP in facilitating export flux in the New Caledonia lagoon (Mari et al., 2007).

484

485 **4 Conclusions**

486 Although physically separated from the surrounding lagoon, TEP formation and
487 breakdown was difficult to tease out in the VAHINE mesocosms where abiotic drivers
488 (turbulence, shear forces, chemical coagulation) and biotic processes (algal and bacterial
489 production and utilization) maintained an apparently constant pool of TEP within the TOC.
490 Total TEP content was generally stable throughout the experimental period of 23 days and
491 comprised ~28% of the TOC in the mesocosms and lagoon with uniform distribution in the
492 three sampled depths of the 15 m deep-water column.

493 TEP concentrations appeared to be impacted indirectly via changes in DIP availability
494 as it was biologically consumed in the mesocosms after fertilization. Thus, declining P
495 availability (low DIP, rapid T_{DIP} , and increased APA) was associated with higher TEP content
496 in all mesocosms. TEP concentrations were also positively associated with net growth rates of
497 two important diazotrophic groups: the DDA *Richelia-Rhizosolenia* (Fig. 6e-f), during P1 and
498 P2 (excluding days 21-23); and UCYN-C diazotrophs which bloomed during P2. High TEP
499 content in the sediment traps during the UCYN-C bloom indicates that TEP may have been
500 part of the organic matrix associated with the large aggregates of UCYN-C that were exported
501 to the sediment traps (Fig. 6g-h).

502 TEP may have also provided bacteria with a rich organic carbon source especially
503 during P2 when higher BP (stimulated by the higher PP) was positively correlated higher TEP
504 concentrations. High production of TEP also occurred in the lagoon water outside the
505 mesocosms on day 23 during the decline of a short-lived dense surface bloom of the
506 diazotrophic *Trichodesmium* (Spungin et al., 2016). Our results emphasize the complexities of
507 the natural system and suggest that to understand the role of compounds such as TEP, and
508 their contribution to the DOC and POC pools, a wider perspective and methodologies should

509 be undertaken to examine and characterize the different components of marine gels (not only
510 carbohydrate-based) (Bar-Zeev et al., 2015; Verdugo, 2012)

511

512 **Author contributions**

513 IBF conceived and designed the investigation of TEP dynamics within the VAHINE project.
514 TM, FVW, IBF, DS, and ER participated in the experiment and performed analyses of
515 samples and data, KTK analysed diazotrophic populations. IBF and DS wrote the manuscript
516 with contributions from all co-authors.

517

518 **Acknowledgements**

519 Many thanks to Sophie Bonnet who created, designed, and successfully executed the
520 VAHINE project .The participation of IBF, DS, and ER in the VAHINE experiment was
521 supported by the German-Israeli Research Foundation (GIF), project number 1133-13.8/2011
522 to IBF,through a collaborative grant to IBF and SB from MOST Israel and the High Council
523 for Science and Technology (HCST)-France, and United States-Israel Binational Science
524 Foundation (BSF) grant No. 2008048 to IBF. Funding for this research was provided by the
525 Agence Nationale de la Recherche (ANR starting grant VAHINE ANR-13-JS06-0002),
526 INSU-LEFE-CYBER program, GOPS, IRD and M.I.O The authors thank the captain and
527 crew of the R/V Alis; the SEOH divers service from the IRD research center of Noumea (E.
528 Folcher, B. Bourgeois and A. Renaud) and from the Observatoire Océanologique de
529 Villefranche-sur-mer (OOV, J.M. Grisoni), the technical service and support of the IRD
530 research center of Noumea. Thanks also to C. Guieu, F. Louis and J.M. Grisoni from OOV for
531 mesocosm design and deployment advice. Special thanks to H. Berthelot and all other
532 participants and PIs of the project for the joint efforts and for making their data available for
533 further analyses and to the reviewers who helped improve the manuscript. This work is in
534 partial fulfillment of the requirements for a PhD thesis for D. Spungin at Bar Ilan University.

535

536

537

538

539 **References**

- 540 Alldredge, A. L., Passow, U., and Logan, B. E.: The abundance and significance of a class of
541 large, transparent organic particles in the ocean., *Deep Sea Research*, 40, 1131-1140, 1993.
- 542 Aminot, A., and K erouel, R.: Dosage automatique des nutriments dans les eaux marines:
543 m ethodes en flux continu, Editions Quae, 2007.
- 544 Azam, F.: Microbial control of oceanic carbon flux: The plot thickens., *Science*, 280, 694-
545 696, 1998.
- 546 Azam, F., and Malfatti, F.: Microbial structuring of marine ecosystems, *Nature Reviews*
547 *Microbiology*, 5, 782-791, 2007.
- 548 Azetsu-Scott, K., and Passow, U.: Ascending marine particles: significance of transparent
549 exopolymer particles (TEP) in the upper ocean., *Limnol. & Oceanogr*, 49, 741-748, 2004.
- 550 Bar-Zeev, E., Berman-Frank, I., Liberman, B., Rahav, E., Passow, U., and Berman, T.:
551 Transparent exopolymer particles: Potential agents for organic fouling and biofilm formation
552 in desalination and water treatment plants, *Desalination and Water Treatment*, 3, 136-142,
553 2009.
- 554 Bar-Zeev, E., Berman, T., Rahav, E., Dishon, G., Herut, B., Kress, N., and Berman-Frank, I.:
555 Transparent exopolymer particle (TEP) dynamics in the eastern Mediterranean Sea, *Marine*
556 *Ecology-Progress Series*, 431, 107-118, 10.3354/meps09110, 2011.
- 557 Bar-Zeev, E., Passow, U., Romero-Vargas Castrill on, S., and Elimelech, M.: Transparent
558 exopolymer particles: from aquatic environments and engineered systems to membrane
559 biofouling, *Environmental science & technology*, 49, 691-707, 2015.
- 560 Beauvais, S., Pedrotti, M. L., Villa, E., and Lemee, R.: Transparent exopolymer particle
561 (TEP) dynamics in relation to trophic and hydrological conditions in the NW Mediterranean
562 Sea, *Marine Ecology-Progress Series*, 262, 97-109, 2003.
- 563 Benavides, M., Moisaner, P. H., Berthelot, H., Dittmar, T., Grosso, O., and Bonnet, S.:
564 Mesopelagic N₂ Fixation Related to Organic Matter Composition in the Solomon and
565 Bismarck Seas (Southwest Pacific), *PLoS ONE*, 10, e0143775,
566 10.1371/journal.pone.0143775, 2015.
- 567 Berman-Frank, I., and Dubinsky, Z.: Balanced growth in aquatic plants: Myth or reality?
568 Phytoplankton use the imbalance between carbon assimilation and biomass production to their
569 strategic advantage, *Bioscience*, 49, 29-37, 1999.
- 570 Berman-Frank, I., Rosenberg, G., Levitan, O., Haramaty, L., and Mari, X.: Coupling between
571 autocatalytic cell death and transparent exopolymeric particle production in the marine
572 cyanobacterium *Trichodesmium*, *Environmental microbiology*, 9, 1415-1422, 2007.
- 573 Berthelot, H., Moutin, T., L'Helguen, S., Leblanc, K., H elias, S., Grosso, O., Leblond, N.,
574 Charri ere, B., and Bonnet, S.: Dinitrogen fixation and dissolved organic nitrogen fueled
575 primary production and particulate export during the VAHINE mesocosm experiment (New
576 Caledonia lagoon), *Biogeosciences*, 12, 4099-4112, 10.5194/bg-12-4099-2015, 2015.
- 577 Biegala, I. C., and Raimbault, P.: High abundance of diazotrophic picocyanobacteria (< 3  m)
578 in a Southwest Pacific coral lagoon, *Aquatic microbial ecology*, 51, 45-53, 2008.
- 579 Bonnet, S., Berthelot, H., Turk-Kubo, K., Fawcett, S., Rahav, E., l'Helguen, S., and Berman-
580 Frank, I.: Dynamics of N₂ fixation and fate of diazotroph-derived nitrogen in a low nutrient

581 low chlorophyll ecosystem: results from the VAHINE mesocosm experiment (New
582 Caledonia), *Biogeosciences*, 12, 19579-19626, doi:10.5194/bgd-12-19579-2015, 2015.

583 Bonnet, S., Moutin, T., Rodier, M., Grisoni, J. M., Louis, F., Folcher, E., Bourgeois, B., Boré,
584 J. M., and Renaud, A.: Introduction to the project VAHINE: Variability of vertical and trophic
585 transfer of diazotroph derived N in the South West Pacific, *Biogeosciences*, doi:10.5194/bg-
586 2015-615, 2016.

587 Brussaard, C., Mari, X., Van Bleijswijk, J., and Veldhuis, M.: A mesocosm study of
588 *Phaeocystis globosa* (Prymnesiophyceae) population dynamics: II. Significance for the
589 microbial community, *Harmful algae*, 4, 875-893, 2005.

590 Capone, D. G.: Marine nitrogen fixation: what's the fuss?, *Curr. Opin. Microbiol.*, 4, 341-348,
591 2001.

592 Duhamel, S., Zeman, F., and Moutin, T.: A dual-labeling method for the simultaneous
593 measurement of dissolved inorganic carbon and phosphate uptake by marine planktonic
594 species, *Limnology and Oceanography-Methods*, 4, 416-425, 2006.

595 Dupouy, C., Neveux, J., Subramaniam, A., Mulholland, M. R., Montoya, J. P., Campbell, L.,
596 Capone, D. G., and Carpenter, E. J.: Satellite captures *Trichodesmium* blooms in the
597 SouthWestern Tropical Pacific., *EOS, Trans American Geophysical Union.*, 81, 13-16, 2000.

598 Engel, A.: The role of transparent exopolymer particles (TEP) in the increase in apparent
599 particle stickiness (α) during the decline of a diatom bloom, *Journal of Plankton Research*, 22,
600 485-497, 2000.

601 Engel, A., and Passow, U.: Carbon and nitrogen content of transparent exopolymer particles
602 (TEP) in relation to their Alcian Blue adsorption, *Marine Ecology Progress Series*, 219, 1-10,
603 2001.

604 Engel, A., Goldthwait, S., Passow, U., and Alldredge, A.: Temporal decoupling of carbon and
605 nitrogen dynamics in a mesocosm diatom bloom, *Limnology and Oceanography*, 47, 3, 753-
606 761, 2002.

607 Engel, A.: Distribution of transparent exopolymer particles (TEP) in the northeast Atlantic
608 Ocean and their potential significance for aggregation processes, *Deep-Sea Research Part I-
609 Oceanographic Research Papers*, 51, 83-92, 2004.

610 Engel, A., Harlay, J., Piontek, J., and Chou, L.: Contribution of combined carbohydrates to
611 dissolved and particulate organic carbon after the spring bloom in the northern Bay of Biscay
612 (North-Eastern Atlantic Ocean), *Continental shelf research*, 45, 42-53, 2012.

613 Eppley, R. W., and Peterson, B. J.: Particulate organic-matter flux and planktonic new
614 production in the deep ocean, *Nature*, 282, 677-680, 10.1038/282677a0, 1979.

615 Falkowski, P. G.: Evolution of the nitrogen cycle and its influence on the biological
616 sequestration of CO₂ in the ocean, *Nature*, 387, 272-275, 1997.

617 Fukao, T., Kimoto, K., and Kotani, Y.: Production of transparent exopolymer particles by four
618 diatom species, *Fisheries science*, 76, 755-760, 2010.

619 García, C., Prieto, L., Vargas, M., Echevarría, F., Garcia-Lafuente, J., Ruiz, J., and Rubin, J.:
620 Hydrodynamics and the spatial distribution of plankton and TEP in the Gulf of Cadiz (SW
621 Iberian Peninsula), *Journal of Plankton Research*, 24, 817-833, 2002.

622 Garcia, N., Raimbault, P., and Sandroni, V.: Seasonal nitrogen fixation and primary
623 production in the Southwest Pacific: nanoplankton diazotrophy and transfer of nitrogen to

624 picoplankton organisms, Marine Ecology-Progress Series, 343, 25-33, 10.3354/meps06882,
625 2007.

626 Grossart, H. P., Simon, M., and Logan, B. E.: Formation of macroscopic organic aggregates
627 (lake snow) in a large lake: The significance of transparent exopolymer particles, plankton,
628 and zooplankton, Limnology and Oceanography, 42, 1651-1659, 1997.

629 Hong, Y., Smith, W. O., and White, A. M.: Studies on transparent exopolymer particles (TEP)
630 produced in the ross sea (antarctica) and by *Phaeocystis antarctica* (prymnesiophyceae),
631 Journal of Phycology, 33, 368-376, 1997.

632 Hoppe, H. G.: Significance of exoenzymatic activities in the ecology of brackish water:
633 measurements by means of methylumbelliferyl-substrates. , Marine Ecology Progress Series,
634 11, 299-308, 1983.

635 Kirchman, D.: Leucine incorporation as a measure of biomass production by heterotrophic
636 bacteria, Handbook of methods in aquatic microbial ecology. Lewis, 509-512, 1993.

637 Knapp, A. N., Fawcett, S. E., Martinez-Garcia, A., Leblond, N., Moutin, T., and Sophie., B.:
638 Nitrogen isotopic evidence for a shift from nitrate- to diazotroph-fueled export production in
639 VAHINE mesocosm experiments, Biogeosciences Discuss., 12, 19901-19939,
640 doi:10.5194/bgd-12-19901-2015, 2015.

641 Leblanc, K., Cornet, V., Caffin, M., Rodier, M., Desnues, A., Berthelot, H., Turk-Kubo, K.,
642 and Heliou, J.: Phytoplankton community structure in the VAHINE mesocosm experiment,
643 Biogeosciences Discuss., doi:10.5194/bg-2015-605, 2016.

644 Logan, B. E., Passow, U., Alldredge, A. L., Grossartt, H.-P., and Simont, M.: Rapid formation
645 and sedimentation of large aggregates is predictable from coagulation rates (half-lives) of
646 transparent exopolymer particles (TEP), Deep Sea Research Part II: Topical Studies in
647 Oceanography, 42, 203-214, 1995.

648 Mari, X., and Burd, A.: Seasonal size spectra of transparent exopolymeric particles (TEP) in a
649 coastal sea and comparison with those predicted using coagulation theory, Marine Ecology-
650 Progress Series, 163, 63-76, 1998.

651 Mari, X., Beauvais, S., Lemée, R., and Pedrotti, M. L.: Non-Redfield C: N ratio of transparent
652 exopolymeric particles in the northwestern Mediterranean Sea, Limnology and
653 Oceanography, 46, 1831-1836, 2001.

654 Mari, X., Kerros, M. E., and Weinbauer, M. G.: Virus attachment to transparent exopolymeric
655 particles along trophic gradients in the southwestern lagoon of New Caledonia, Applied and
656 Environmental Microbiology, 73, 5245-5252, 10.1128/aem.00762-07, 2007.

657 Mohr, W., Grosskopf, T., Wallace, D. W., and LaRoche, J.: Methodological underestimation
658 of oceanic nitrogen fixation rates, PLOS one, 5, e12583, 2010.

659 Moisander, P. H., Serros, T., Paerl, R. W., Beinart, R. A., and Zehr, J. P.:
660 Gammaproteobacterial diazotrophs and nifH gene expression in surface waters of the South
661 Pacific Ocean, The ISME journal, 8, 1962-1973, 2014.

662 Moutin, T., Thingstad, T. F., Van Wambeke, F., Marie, D., Slawyk, G., Raimbault, P., and
663 Claustre, H.: Does competition for nanomolar phosphate supply explain the predominance of
664 the cyanobacterium *Synechococcus*?, Limnology and Oceanography, 47, 1562-1567, 2002.

665 Moutin, T., Van Den Broeck, N., Beker, B., Dupouy, C., Rimmelin, P., and Le Bouteiller, A.:
666 Phosphate availability controls *Trichodesmium* spp. biomass in the SW Pacific Ocean, Marine
667 Ecology-Progress Series, 297, 15-21, 2005.

668 Mulholland, M. R., and Capone, D. G.: The nitrogen physiology of the marine N₂-fixing
669 cyanobacteria *Trichodesmium* spp, Trends in plant science, 5, 148-153, 2000.

670 Ortega-Retuerta, E., Reche, I., Pulido-Villena, E., Agustí, S., and Duarte, C. M.: Uncoupled
671 distributions of transparent exopolymer particles (TEP) and dissolved carbohydrates in the
672 Southern Ocean, Marine chemistry, 115, 59-65, 2009.

673 Passow, U., and Alldredge, A. L.: A dye binding assay for the spectrophotometric
674 measurement of transparent exopolymer particles (TEP), Limnol. & Oceanogr, 40, 1326-
675 1335, 1995.

676 Passow, U.: Transparent exopolymer particles (TEP) in aquatic environments, Progress in
677 Oceanography, 55, 287-333, 2002.

678 Postgate, J. R., and Eady, R. R.: The evolution of biological nitrogen fixation, in: Nitrogen
679 Fixation: One Hundred Years After, edited by: Bothe, H., DeBruijn, F. J., Newton, W.E,
680 Gustav Fischer, Stuttgart, 31-40., 1988.

681 Prieto, L., Navarro, G., Cozar, A., Echevarria, F., and García, C. M.: Distribution of TEP in
682 the euphotic and upper mesopelagic zones of the southern Iberian coasts, Deep Sea Research
683 Part II: Topical Studies in Oceanography, 53, 1314-1328, 2006.

684 Radić, T., Degobbi, D., Fuks, D., Radić, J., and Đakovac, T.: Seasonal cycle of transparent
685 exopolymer particles' formation in the northern Adriatic during years with (2000) and without
686 mucilage events (1999), Fresenius environmental bulletin, 14, 224-230, 2005.

687 Rahav, E., Bar-Zeev, E., Ohayion, S., Elifantz, H., Belkin, N., Herut, B., Mulholland, M. R.,
688 and Berman-Frank, I. R.: Dinitrogen fixation in aphotic oxygenated marine environments,
689 Frontiers in Microbiology, 4, 10.3389/fmicb.2013.00227, 2013.

690 Rahav, E., Herut, B., Mulholland, M. R., Belkin, N., Elifantz, H., and Berman-Frank, I.:
691 Heterotrophic and autotrophic contribution to dinitrogen fixation in the Gulf of Aqaba,
692 Marine Ecology Progress Series, 522, 67-77, 2015.

693 Rochelle-Newall, E., Torreton, J.-P., Mari, X., and Pringault, O.: Phytoplankton-
694 bacterioplankton coupling in a subtropical South Pacific coral reef lagoon, Aquatic Microbial
695 Ecology, 50, 221, 2008.

696 Rodier, M., and Le Borgne, R.: Population dynamics and environmental conditions affecting
697 *Trichodesmium* spp. (filamentous cyanobacteria) blooms in the south-west lagoon of New
698 Caledonia, Journal of Experimental Marine Biology and Ecology, 358, 20-32,
699 10.1016/j.jembe.2008.01.016, 2008.

700 Rodier, M., and Le Borgne, R.: Population and trophic dynamics of *Trichodesmium thiebautii*
701 in the SE lagoon of New Caledonia. Comparison with *T. erythraeum* in the SW lagoon,
702 Marine Pollution Bulletin, 61(7-12), 349-359, 10.1016/j.marpolbul.2010.06.018, 2010.

703 Smith, D. C., and Azam, F.: A simple, economic method for measuring bacterial protein
704 synthesis rates in seawater using ³H-leucine Mar. Microb. Food Webs, 6, 107-114, 1992.

705 Spungin, D., Pfreundt, U., Berthelot, H., Bonnet, S., Al-Roumi, D., Natale, F., Hess, W. R.,
706 Bidle, K. D., and Berman-Frank, I.: Mechanisms of *Trichodesmium* bloom demise within the

707 New Caledonia Lagoon during the VAHINE mesocosm experiment, *Biogeosciences Discuss.*,
708 doi:10.5194/bg-2015-613, 2016.

709 Stam, H., Stouthamer, A. H., and van Verseveld, H. W.: Hydrogen metabolism and energy
710 costs of nitrogen fixation, *FEMS Microbiology Reviews*, 46, 73-92, 1987.

711 Stoderegger, K. E., and Herndl, G. J.: Production of exopolymer particles by marine
712 bacterioplankton under contrasting turbulence conditions, *Marine Ecology Progress Series*,
713 189, 9-16, 1999.

714 Tedetti, M., Marie, L., Röttgers, R., Rodier, M., Van Wambeke, F., Helias, S., Caffin, M.,
715 Cornet-Barthaux, V., and Dupouy, C.: Evolution of dissolved and particulate chromophoric
716 materials during the VAHINE mesocosm experiment in the New Caledonian coral lagoon
717 (South West Pacific), *Biogeosciences Discuss.*, 12, 17453-17505, doi:10.5194/bg-12-17453-
718 2015, 2015.

719 Thurman, E.: *Organic Geochemistry of Natural Waters*, Martinus Nijhoff/Dr W. Junk
720 Publishers, Dordrecht, 1985.

721 Turk-Kubo, K., Frank, I., Hogan, M., Desnues, A., Bonnet, S., and Zehr, J.: Diazotroph
722 community succession during the VAHINE mesocosm experiment (New Caledonia lagoon),
723 *Biogeosciences*, 12, 7435-7452, doi:10.5194/bg-12-7435-2015, 2015.

724 Urbani, R., Magaletti, E., Sist, P., and Cicero, A. M.: Extracellular carbohydrates released by
725 the marine diatoms *Cylindrotheca closterium*, *Thalassiosira pseudonana* and *Skeletonema*
726 *costatum*: Effect of P-depletion and growth status, *Science of the Total Environment*, 353,
727 300-306, 2005.

728 Van Wambeke, F., Pfreundt, U., Barani, A., Berthelot, H., Moutin, T., Rodier, M., Hess,
729 W.R., and S, B.: Heterotrophic bacterial production and metabolic balance during the
730 VAHINE mesocosm experiment in the New Caledonia lagoon, *Biogeosciences*, 12, 19861-
731 19900, doi:10.5194/bg-12-19861-2015, 2015.

732 Verdugo, P., and Santschi, P. H.: Polymer dynamics of DOC networks and gel formation in
733 seawater, *Deep Sea Research Part II: Topical Studies in Oceanography*, 57, 1486-1493, 2010.

734 Verdugo, P.: Marine microgels, *Annual review of marine science*, 4, 375-400, 2012.

735 Villacorte, L. O., Ekowati, Y., Calix-Ponce, H. N., Schippers, J. C., Amy, G. L., and
736 Kennedy, M. D.: Improved method for measuring transparent exopolymer particles (TEP) and
737 their precursors in fresh and saline water, *Water research*, 70, 300-312, 2015.

738 Wood, A., and Van Valen, L.: Paradox lost? On the release of energy-rich compounds by
739 phytoplankton, *Microbial Food Webs*, 4, 103-116, 1990.

740 Wurl, O., Miller, L., and Vagle, S.: Production and fate of transparent exopolymer particles in
741 the ocean, *Journal of Geophysical Research: Oceans (1978-2012)*, 116, 2011.

742 Zehr, J. P., and Kudela, R. M.: Nitrogen Cycle of the Open Ocean: From Genes to
743 Ecosystems, in: *Annual Review of Marine Science*, Vol 3, *Annual Review of Marine Science*,
744 197-225, 2011.

745 Zhou, J., Mopper, K., and Passow, U.: The role of surface-active carbohydrates in the
746 formation of transparent exopolymer particles by bubble adsorption of seawater, *Limnology*
747 *and Oceanography*, 43, 1860-1871, 1998.

748 Ziervogel, K., D'souza, N., Sweet, J., Yan, B., and Passow, U.: Natural oil slicks fuel surface
749 water microbial activities in the northern Gulf of Mexico, *Frontiers in microbiology*, 5, 2014.

750

751

752 **Figure legends**

753 **Figure 1.** Temporal changes in transparent exopolymeric particle (TEP) concentrations (μg
754 GX L^{-1}) during the VAHINE mesocosm experiment. Data shown are from daily sampling of
755 three depths (1, 6, 12 m) in each mesocosm. Data was analyzed according to the characterized
756 phases of the experiment based on the diazotrophic communities that developed in the
757 mesocosms (Turk-Kubo et al., 2015) and biogeochemical characteristics (Bonnet et al., 2015).
758 **a.** Mesocosm 1 (M1) **b.** Mesocosm 2 (M2), **c.** Mesocosm 3 (M3), **d.** samples from the lagoon
759 waters outside of the mesocosms (O). Phases: P0= days 2-4, P1= days 5-14, P2= days 15-23.
760 Linear regressions (Pearson) of TEP for each of the phases are designated by a solid line, only
761 when significant. Pearson correlations coefficients and significant values ($p < 0.05$) are
762 represented in bold in Table S1.

763 **Figure 2.** Total content of transparent exopolymeric particles (TEP) per mesocosm and in the
764 lagoon waters surrounding the mesocosms. The average amount in $\text{g GX mesocosm}^{-1}$ for the
765 two periods of the experiment after DIP fertilization was calculated from the total daily
766 amount based on concentrations measured at three depths and integrated for the specific
767 volume per mesocosm or for an equivalent volume of lagoon water. Averages are represented
768 in boxplots as a function of two different phases: P1 = days 5-14 and P2 = days 15-23. Red
769 (mesocosm 1 - M1), blue (mesocosm 2- M2), green (mesocosm - M3) and black (Outside
770 lagoon O). Straight lines within the boxes mark the median. No significant differences were
771 observed between the phases or between the three mesocosms and the outside lagoon
772 (Kruskal-Wallis non-parametric analysis of variance; $p > 0.05$).

773 **Figure 3.** Relationships between the concentration of transparent exopolymeric particles
774 (TEP), ($\mu\text{g GX L}^{-1}$) and **a.** dissolved inorganic phosphorus DIP ($\mu\text{mol L}^{-1}$), **b.** turnover time of
775 DIP - T_{DIP} (d) and **c.** alkaline phosphatase activity (APA), ($\text{nmol L}^{-1} \text{h}^{-1}$) in the three
776 mesocosms (M1-red; M2-blue; M3-green) during phase 2 (days 15-23). For a and b Pearson
777 linear regressions yielded an $R^2 = 0.54$, $n = 23$ (TEP/DIP) and an $R^2 = 0.52$, $n = 26$
778 (TEP/ T_{DIP}), and for c. Log-transformed ($\log(\text{TEP}) / \log(\text{APA})$) with $R^2 = 0.68$, $n = 25$. All
779 correlations were significant ($p < 0.05$). Error bars represent ± 1 standard deviation.

780 **Figure 4. a.** Temporal dynamics of TEP carbon concentrations (TEP-C, μM) in relationship
781 to the average total organic carbon (TOC), ($\mu\text{g L}^{-1}$), (thin black line) in the mesocosms (M1-
782 red dots, M2-blue dots, M3-green dots, and black dots- Outside waters (O). Black solid line
783 designates TEP-C averaged for the three mesocosms (thick black line). TEP-C was measured

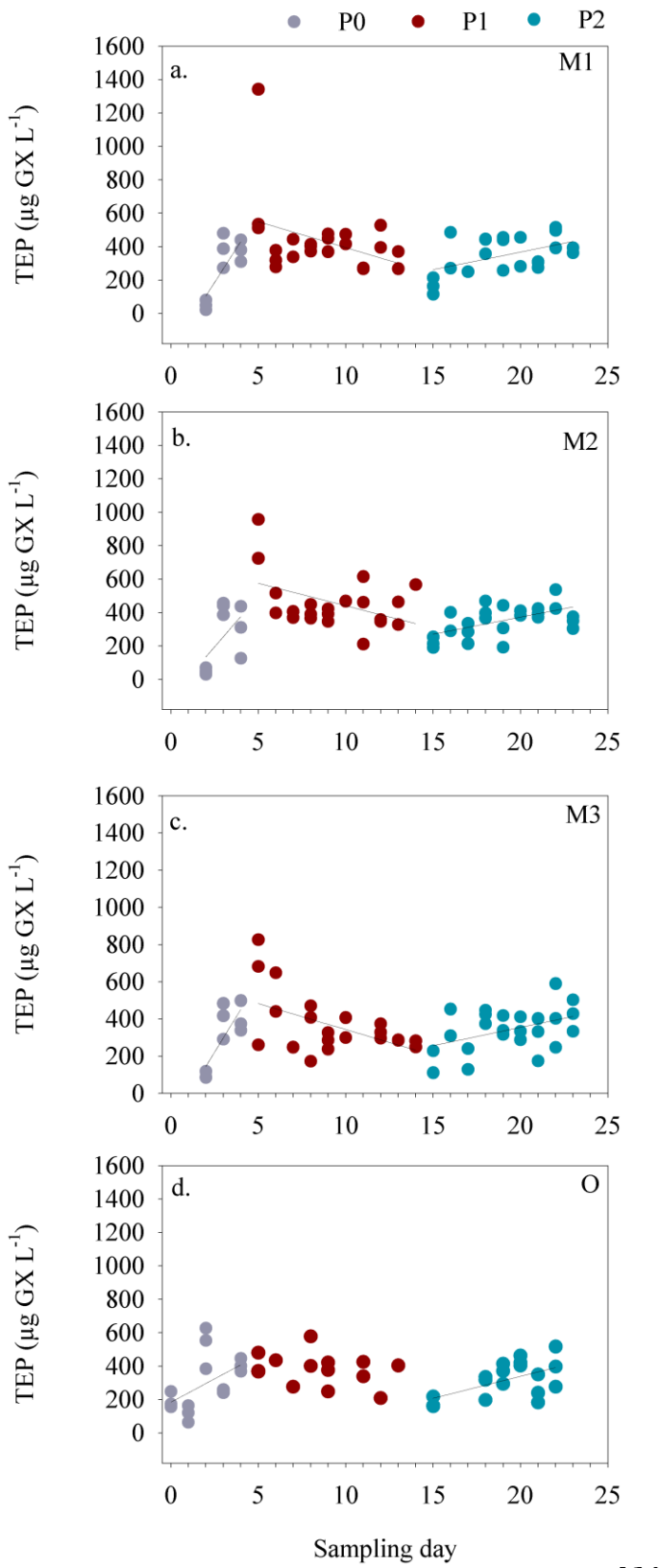
784 from 6 m depths and calculated according to Engel (2000). **b.** Temporal changes in the
785 percent of TEP-C from TOC (%) in mesocosms (green dots), and %TEP-C in the lagoon
786 waters (Out), (black dots). **c.** Relationship between TEP concentrations ($\mu\text{g GX L}^{-1}$) and TOC
787 ($\mu\text{mole L}^{-1}$), during phase 2 (days 15-23) for Mesocosm 1 (M1, red dots), Mesocosm 2 (M2,
788 blue dots), Mesocosm 3 (M3, green dots). Significant correlations were observed (Pearson)
789 for all mesocosms. $R^2 = 0.75\text{-M1}$, 0.73-M2 , and 0.58-M3 respectively, $n=7\text{-8}$, $p < 0.05$. All
790 statistics are detailed in Table S2, ($p=0.05$, $n= 7\text{-8}$). Error bars represent ± 1 standard
791 deviation.

792 **Figure 5.** Relationship between heterotrophic bacterial production (BP), ($\text{ng C L}^{-1} \text{ h}^{-1}$) and
793 TEP concentrations ($\mu\text{g GX L}^{-1}$) during phase 2 (days 15-23) when BP increased following
794 the enhanced PP (Van Wambeke et al., 2015), for Mesocosm 1 (M1, red dots), Mesocosm 2
795 (M2, blue dots), Mesocosm 3 (M3, green dots). Pearson's linear regressions yielded $R^2 = 0.57$
796 for M1, 0.42 for M2, and 0.56 for M3 respectively. Significant correlations were observed for
797 all mesocosms and are detailed in Table S2. Error bars represent ± 1 standard deviation.

798 **Figure 6.** Temporal changes in TEP concentrations and Het-1 net growth rates (d^{-1}), (gray
799 triangles) for **a.** Mesocosm 1 (M1) **b.** Mesocosm 2 (M2), **c.** Mesocosm 3 (M3). TEP
800 concentrations were averaged from the three depths sampled per mesocosm (green circles).
801 Het-1 net growth rates were calculated based on changes of *nifH* copies L^{-1} (Turk-Kubo et al.,
802 2015) measured every other day. **d.** Relationship between TEP concentrations ($\mu\text{g GX L}^{-1}$)
803 and Het-1 growth rate (d^{-1}) for all three mesocosms. Significant correlations were observed
804 (Pearson) from all mesocosms together. $R^2 = 0.60$, $p = 0.0001$, $n = 19$. Error bars represent \pm
805 1 standard deviation. **e-f.** Epifluorescent microscopical images of the diatom-diazotroph
806 association *Richelia-Rhizosolenia* identified by Het-1 abundance. Images by V. Cornet-
807 Barthaux. **g-h.** the diazotroph UCYN-C which bloomed and formed large aggregates
808 (comprised also of TEP) that enhanced vertical flux and export production during P2. Images
809 by S. Bonnet.

810

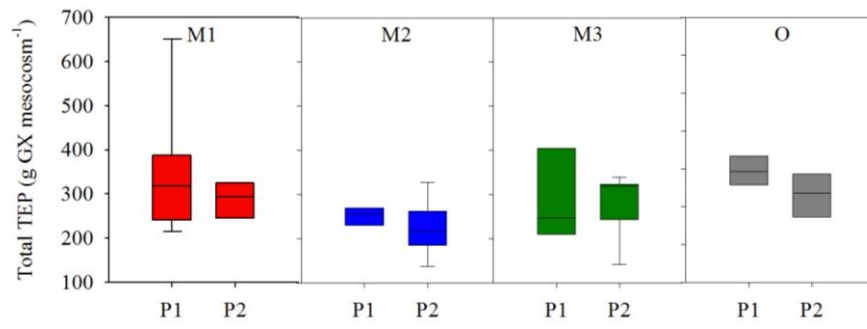
811 **Figure 1**



836

837 **Figure 2**

838



844

845

846

847

848

849

850

851

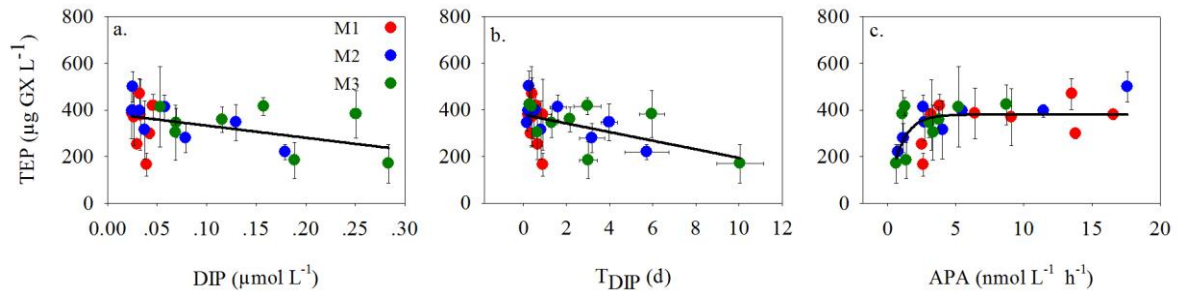
852

853

854 **Figure 3**

855

856



857

858

859

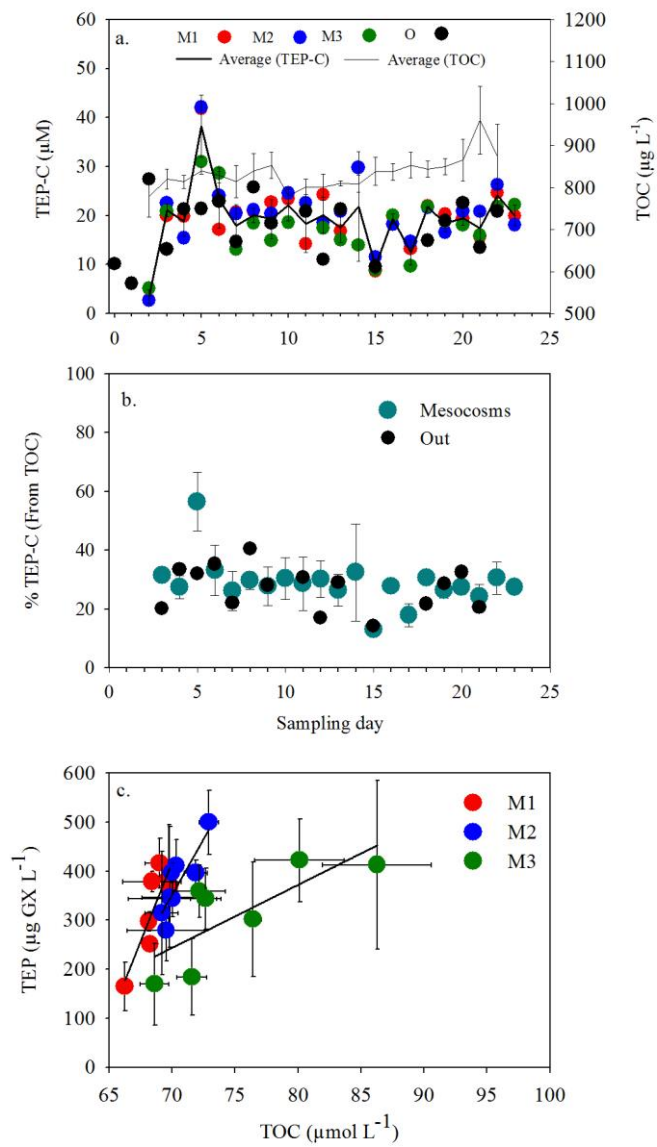
860

861

862 **Figure 4**

863

864



882

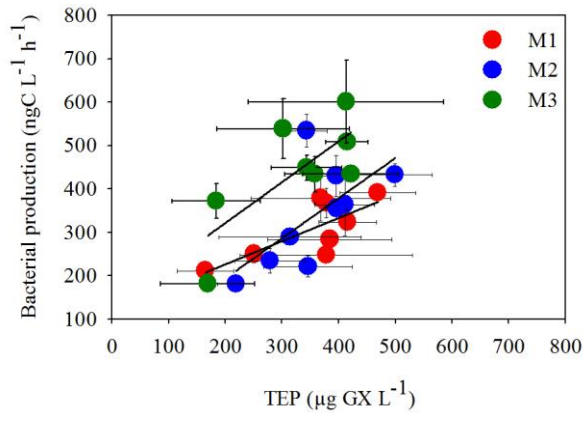
883

884

885 **Figure 5**

886

887



888

889

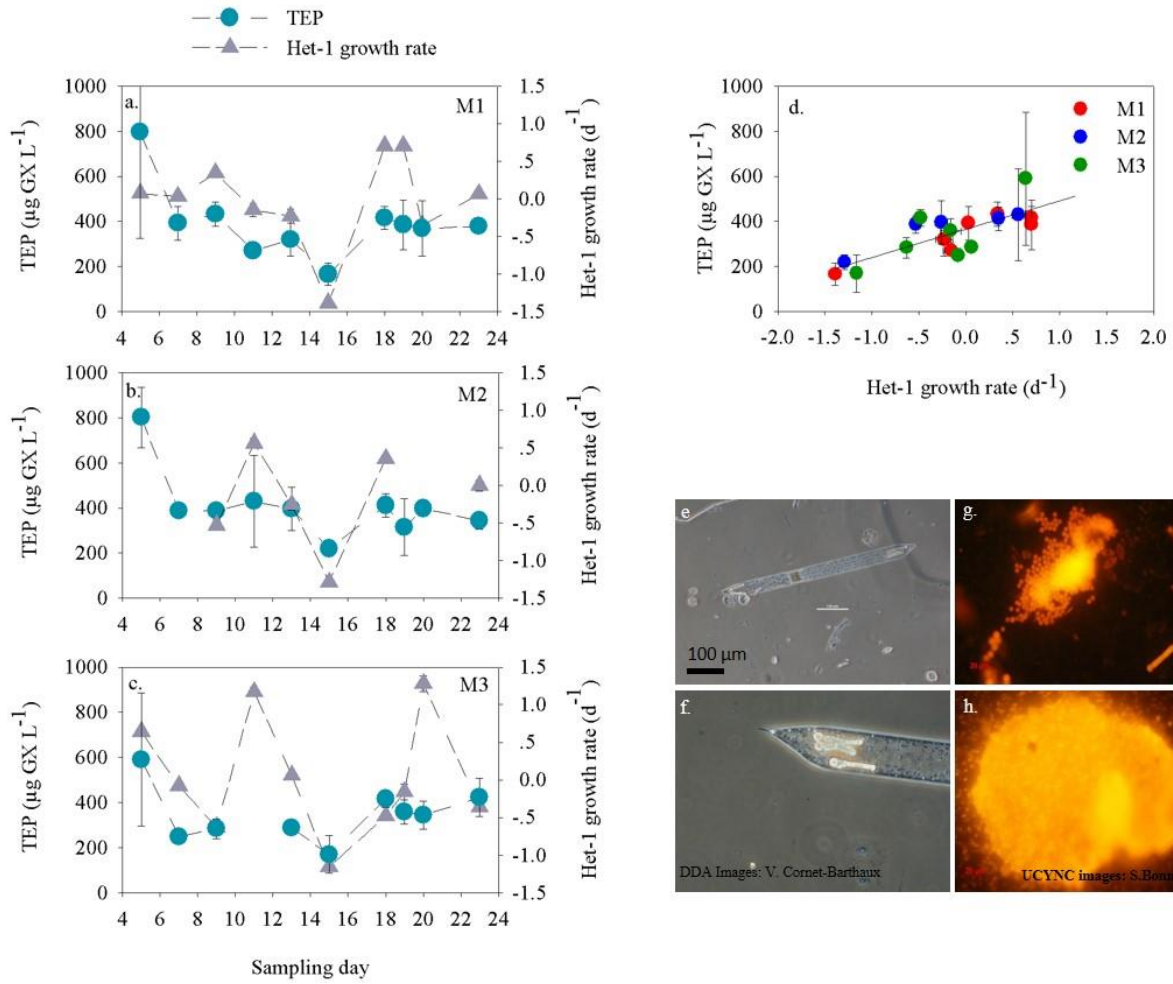
890

891

892 **Figure 6**

893

894



895

896

897

898

899

900